

Design and characterization of SiC varactor-based phase shifters

*Original*

Design and characterization of SiC varactor-based phase shifters / Quaglia, Roberto; Camarchia, Vittorio; C. M., Andersson; Pirola, Marco; C., Fager; D., Kuylenstierna. - STAMPA. - Unico:(2012), pp. 1277-1280. ( Microwave Conference (EuMC), 2012 42nd European Amsterdam Oct. 29 2012-Nov. 1 2012).

*Availability:*

This version is available at: 11583/2518973 since:

*Publisher:*

IEEE - INST ELECTRICAL ELECTRONICS ENGINEERS INC

*Published*

DOI:

*Terms of use:*

This article is made available under terms and conditions as specified in the corresponding bibliographic description in the repository

*Publisher copyright*

(Article begins on next page)

# Design and characterization of SiC varactor-based phase shifters

Roberto Quaglia\*, Vittorio Camarchia\*, Christer M. Andersson†, Marco Pirola\*, Christian Fager† and Dan Kuylenstierna†

\*Dept. of Electronics and Telecommunications, Politecnico di Torino, I-10129 Torino, Italy. Email: roberto.quaglia@polito.it

† Dept. of Microtechnology and Nanoscience, MC2, Chalmers University of Technology, SE-412 96 Gothenburg, Sweden

**Abstract**—Design and realization of two continuously tunable phase shifters for 1.4 GHz band is presented. Both circuits are based on SiC varactors, conceived to enable high-voltage, high-power operation, and suitable for application in the transmitter chain of reconfigurable radios. Experimental characterization shows, for the loaded line phase shifter, 74° maximum phase shift with insertion loss lower than 1 dB, and, for the reflective phase shifter, 90° maximum phase shift and insertion loss lower than 0.6 dB.

## I. INTRODUCTION

The increasing demand of multi-mode, multi-standard radios is driving toward the development of fully reconfigurable microwave front ends, based on electronically tunable networks. When placed in the transmitter chain, these networks must be able to handle high power, and their RF losses and DC power consumption crucially affect the overall system efficiency. Among others examples, phase shifters are widely adopted in reconfigurable microwave circuits, that find several applications, e.g. in phased array antennas or phase compensation networks for advanced power amplifiers. Here we present the design and characterization of two phase shifters for L-band based on reversely biased SiC varactor diodes: the first is a “loaded line phase shifter” (see Fig. 1a), the second a “reflective phase shifter” (see Fig. 1b). With respect to other

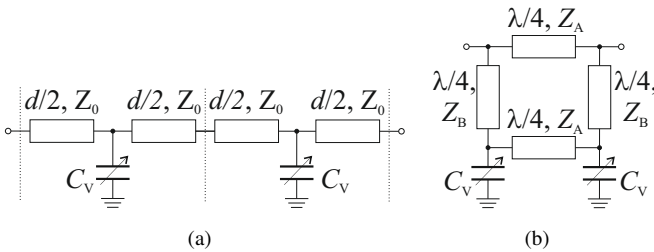


Fig. 1. Circuit diagrams of the designed phase shifters: loaded line phase shifter (a) and reflective phase shifter (b).

possible solutions for the realization of tunable impedances, e.g. p-i-n diodes [1], ferroelectric varactors [2], MEMS [3], SiC varactor diodes show promising performances. In fact, not only they can be continuously controlled practically without current absorption, but can handle high voltage swing, and high power. Given the recent development of these components, it is important to experimentally assess their performances: in this work, for the first time as the authors’ knowledge goes, SiC varactor based phase shifters are designed and characterized.

## II. DESIGN

Phase shifters are two port circuits that introduce a variable phase delay  $\phi(V_C)$ , i.e. the phase of  $S_{21}$ , according to the control voltage  $V_C$ . The phase delay is typically assigned in relative rather absolute terms, expressing it with respect to a reference value. It is in fact introduced  $\Delta\phi(V_C) = \phi(V_C) - \phi(V_0)$ , where the reference phase factor is  $\phi(V_0)$ . The two most important figures of merit to evaluate and compare phase shifter performances are  $\Delta\phi_M$ , the maximum value reached by  $\Delta\phi(V)$  as a function of the control voltage, and the Insertion Loss (IL), namely  $IL = -20\log_{10}|S_{21}|$ . These two key features can be simultaneously taken into account introducing a unique figure of merit  $F_{\Delta\phi}$ , defined as:

$$F_{\Delta\phi} = \frac{|\Delta\phi_M|}{\max\{IL(V_C), IL(V_0)\}}. \quad (1)$$

To enable the adoption of phase shifters in high-power, high-voltage circuits, the selection of the tunable components (i.e. the varactors) is led considering that the target devices must be able to manage high-voltage swing, achieving at the same time a reasonable capacitance tuning ratio. The exhibited

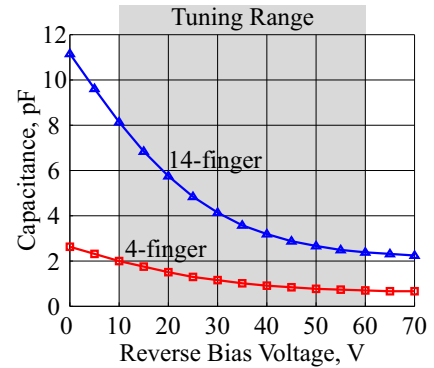


Fig. 2. Capacitance vs. reverse voltage behavior of 4-finger (blue line with dots) and 14-finger (red line with squares) SiC diode varactors.

quality factor must also be considered, to avoid performance degradation due to phase shifter losses. In this work, we present two phase shifters designed at 1.4 GHz, the center frequency of the L-Band, implementing a loaded line, and a reflective scheme respectively. We based our designs on SiC Schottky diodes fabricated at Chalmers University [4].

The device doping profile has been optimized to increase the tunable range, in other words to ensure a capacitance *vs.* control voltage spreading over a large range of the reverse voltage. Moreover, to maximize the varactor quality factor, a self-aligned process for anode deposition, together with inter-digitated layout, have been adopted. Fig.2 shows the capacitance *vs.* voltage curves of the two available varactor sizes, with 4 and 14 fingers respectively. The quality factor, experimentally identified through small signal measurements at frequencies close to 1.4 GHz, is around 20 and 160, at zero and punch-through voltage [4], respectively.

In phase shifter based on varactor diodes, it is important to ensure that they are never driven in forward conduction condition, and the varactor bias voltage must be chosen accordingly. This constraint reduces the varactor, and consequently, phase shifter voltage tuning range. In the present work, varactors are tuned in a range from 10 to 60 V. The minimum value, 10 V, allows a considerable voltage swing on the varactor (i.e. 20 V), see Fig.2, while the maximum value has been selected since, despite the reverse breakdown is above 100 V, the capacitance modulation is negligible for reverse voltage exceeding this value. The reference voltage  $V_0$  is set to 60 V, hence  $\Delta\phi(V_C) = \phi(V_C) - \phi(60 \text{ V})$ , and  $\Delta\phi_M = \Delta\phi(10 \text{ V})$  represents the maximum phase shifting.

A scalable, accurate and reliable non-linear model for these devices have been developed at the Chalmers University, and already successfully adopted in other designs [5], [6]. It is based on a non-linear capacitance and series resistance, for the intrinsic part, and it accounts for the extrinsic parasitic effects of bonding and mounting pads.

The microstrip phase shifters are realized on a Taconic substrate, with dielectric constant of 2.33, substrate height of  $380 \mu\text{m}$ , and copper metalization film of  $35 \mu\text{m}$  thickness. The microstrip circuit is placed on aluminum carrier, to allow the mounting of the varactors, that are connected through bonding wires to the access lines.

#### A. Loaded Line Phase Shifter

The scheme of the varactor loaded line phase shifter is shown in Fig. 1a: it consists of cascaded T-sections, each of them containing a shunt varactor comprised between two transmission line segments. As a result, a synthetic transmission line is obtained, whose phase constant, and as consequence phase delay, depends on the varactor capacitance  $C_V$ , and thus on the control voltage. In fact, for a periodically loaded transmission line, the length of the inserted lines, is small with respect to  $\lambda/4$ , the phase constant  $\beta_V$  differs from the unloaded line phase constant  $\beta_0$  according to:

$$\beta_V = \beta_0 \sqrt{1 + \frac{C_V}{\mathcal{E}d}} \quad (2)$$

where  $d$  is the T-section physical length, and  $\mathcal{E}$  is the per unit length capacitance of the line, that can be expressed as:

$$\mathcal{E} = \frac{\sqrt{\epsilon_{r,\text{eff}}}}{Z_0 c} \quad (3)$$

where  $\epsilon_{r,\text{eff}}$  is the effective permittivity of the physical transmission line, while  $Z_0$  is its characteristic impedance, and  $c$  is the light speed in vacuum. On the other hand, also the equivalent line impedance  $Z_t$  results to be dependent on  $C_V$ :

$$Z_t = Z_0 \left[ \frac{C_V}{\mathcal{E}d} - 1 \right]^{-\frac{1}{2}}. \quad (4)$$

This leads to a trade-off between the mismatch, negatively affecting the insertion loss IL, and maximum phase shift. To maintain IL reasonably low, the varactor size can be chosen so that  $Z_t$  is equal to the system impedance, i.e.  $50 \Omega$ , when  $C_V$  assumes values close to the middle of its excursion.

It must be noticed that a solution of the circuit for the optimization of  $F_{\Delta\phi}$  strongly depends on the choice of  $d$  and  $Z_0$ : at the same time, turning to a microstrip implementation, the strip losses are themselves depending on  $Z_0$ . As a consequence, the present design is based on preliminary simulations in the Agilent ADS CAD suite to identify the varactor size, and the 4-finger SiC varactor (whose characteristic is shown in Fig.2) is chosen. Then, an accurate optimization of the phase shifter is carried out to maximize the performances in terms of  $F_{\Delta\phi}$  at the design frequency. The circuit is fabricated with in-house facilities, so only two phase shifter sections are inserted, to minimize the mounting issues. The varactors are commonly biased through an RF choke inductor connected to the microstrip line, and DC decoupling capacitors are inserted at the phase shifter ports, see schematic in Fig.3 and picture in Fig.4.

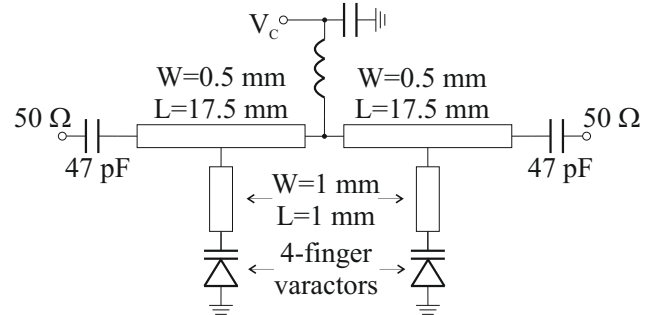


Fig. 3. Complete schematic of the designed loaded line phase shifter.

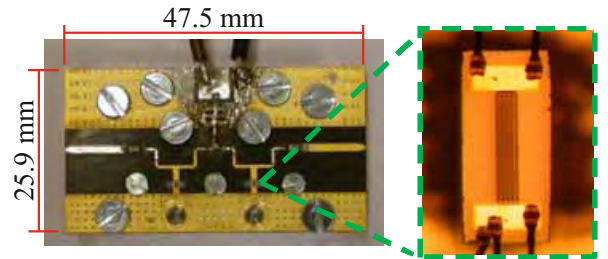


Fig. 4. Picture of the designed loaded line phase shifter. The mounted 4-finger varactor is highlighted.

### B. Reflective Phase Shifter

The reflective phase shifter scheme is shown in Fig. 1b: it is based on a 90-degree 3dB coupler (a branch line in the present work, with  $Z_A = 50\ \Omega$ ,  $Z_B = 35\ \Omega$ ) loaded by two identical varactors. The variation of the varactors capacitance vs. voltage leads to a phase shift in the transmission path. The amount of phase shifting can be approximated [7], considering ideal components, as:

$$\Delta\phi_M = 2 \left[ \tan^{-1} \left( \frac{1}{\omega Z_0 C_{V_m}} \right) - \tan^{-1} \left( \frac{1}{\omega Z_0 C_{V_M}} \right) \right] \quad (5)$$

where  $\omega = 2\pi f$ , and  $C_{V_m}$ ,  $C_{V_M}$  are the minimum and maximum varactor capacitance, respectively. Considering that the Q-factor is the same for 4- and 14-finger varactor, we can assume that the insertion loss of the phase shifter will be comparable for the two solutions. Consequently, the choice

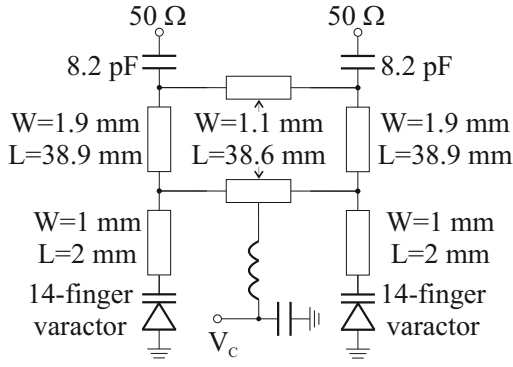


Fig. 5. Complete schematic of the designed reflective phase shifter.

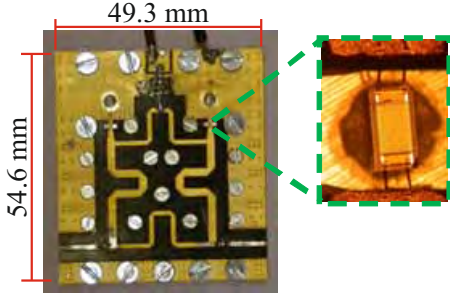


Fig. 6. Picture of the designed reflective phase shifter. The mounted 14-finger varactor is highlighted.

of the varactor is carried out to achieve the maximum  $\Delta\phi_M$  at 1.4 GHz. The capacitance variation of the 4-finger varactor is between 0.7 pF and 2 pF, corresponding to a maximum phase shift of  $49^\circ$ . Since the 14-finger varactor exploits a 2.2 pF to 8.1 pF capacitance range, with  $61^\circ$  phase shifting, it has been adopted. The branch line is realized with a distributed topology that gives lower losses with respect to a semi-lumped solutions. The final circuit and layout have been extensively and accurately optimized through CAD simulations, see complete circuit and picture of the microstrip realization in Fig. 5 and Fig. 6 respectively.

### III. CHARACTERIZATION

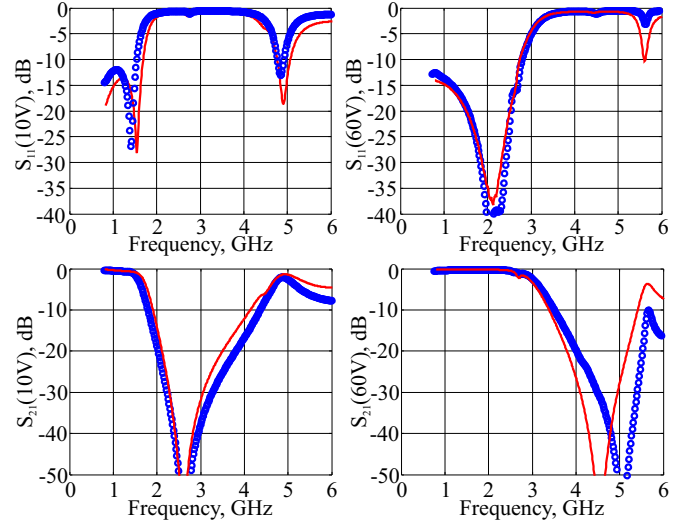


Fig. 7. Scattering characterization of the loaded line phase shifter, for  $V_C = 10\text{ V}$  and  $V_C = 60\text{ V}$ . Red line: simulations, blue circles: measurements.

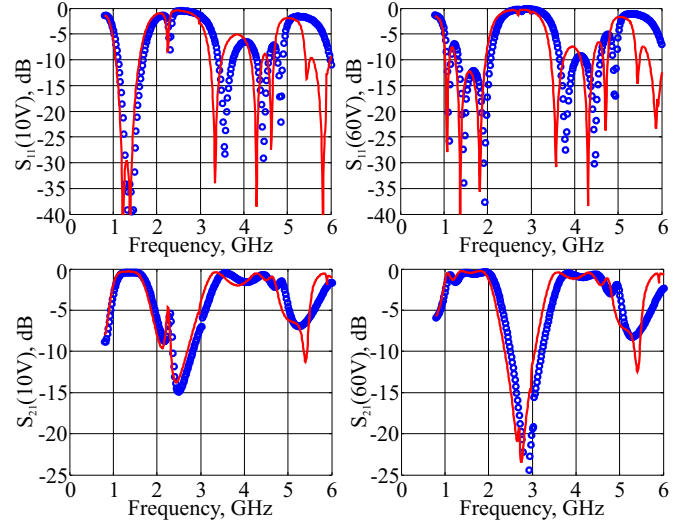


Fig. 8. Scattering characterization of the reflective phase shifter, for  $V_C = 10\text{ V}$  and  $V_C = 60\text{ V}$ . Red line: simulations, blue circles: measurements.

The RF access lines to the phase shifters are conceived to fit the launchers of an Anritsu/Wiltron Test Fixture [8], and the bench is RF calibrated through a thru-reflect-line de-embedding procedure [9]. The circuits are characterized by scattering measurements from 0.8 GHz to 6 GHz, sweeping the control voltages  $V_C$  from 10 V to 60 V. Fig. 7 and Fig. 8 show the scattering parameters of the two phase shifters for  $V_C$  sets to 10 V and 60 V: the agreement between measurements and simulations results good also for out-of-band frequencies. Fig. 9 and Fig. 10 show, for the loaded line and reflective phase shifters, the simulated and measured  $\Delta\phi_M$  and IL vs. frequency: even in this case the agreement is rather good.

The measured return loss at 1.4 GHz results always better

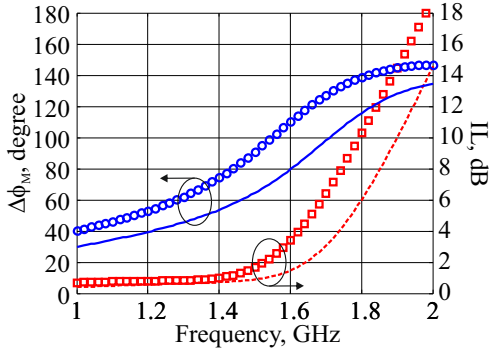


Fig. 9. Frequency behaviour of the loaded line phase shifter.  $\Delta\phi_M$  (blue line: simulations, blue circles: measurements) and IL (red dashed line: simulations, red squares: measurements).

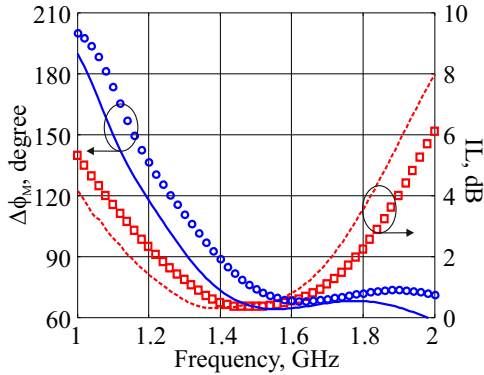


Fig. 10. Frequency behaviour of the reflective phase shifter.  $\Delta\phi_M$  (blue line: simulations, blue circles: measurements) and IL (red dashed line: simulations, red squares: measurements).

than 16 dB for both phase shifters. The measured  $F_{\Delta\phi}$  of both phase shifters is compared in Fig. 11, while Fig. 12 shows the  $\Delta\phi(V_C)$  at 1.4 GHz. For both phase shifters, the  $F_{\Delta\phi}$  has

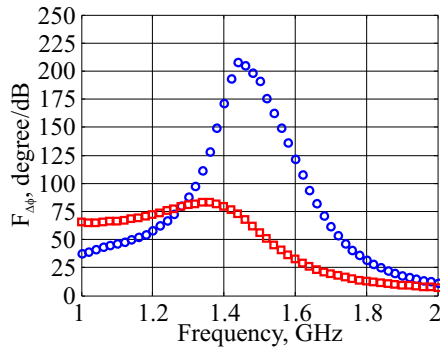


Fig. 11. Measured  $F_{\Delta\phi}$  vs. frequency behaviour of the loaded line phase shifter (red square) and of the reflective phase shifter (blue circles).

its maximum around 1.4 GHz: in the loaded line case, this derives from the combination of the low-pass behaviour of the loaded line structure and the increasing  $\Delta\phi_M$  vs. frequency.

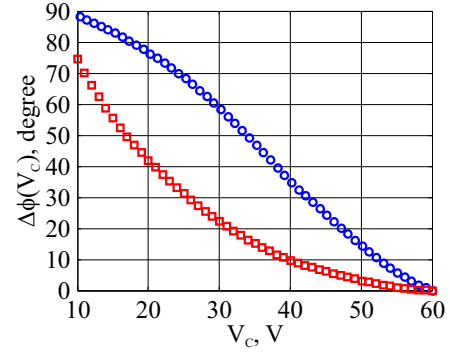


Fig. 12. Measured  $\Delta\phi$  vs. applied voltage behaviour, at 1.4 GHz, of the loaded line phase shifter (red square) and of the reflective phase shifter (blue circles).

In the reflective phase shifter, IL is minimized at 1.4 GHz, while the phase shift is decreasing vs. frequency. For both implementations, some discrepancies between measurements and simulations can be ascribed to the lack of uniformity of SiC varactor substrates that affects the diode repeatability.

#### IV. CONCLUSION

The design and characterization of two SiC varactor based phase shifters for L-band is presented: a loaded line and a reflective implementation. At 1.4 GHz, the loaded line phase shifter exhibits  $74^\circ$  of differential phase shift, with insertion loss lower than 1 dB. At the same center band frequency, the reflective phase shifter presents a  $90^\circ$  phase shift, with less than 0.6 dB insertion loss. Thanks to the adopted SiC varactors, the designed phase shifters are enabling components for the design of high power microwave reconfigurable networks.

#### REFERENCES

- [1] H. Takasu, et.al., "Ka-band low loss and high power handling GaAs PIN diode MMIC phase shifter for reflected-type phased array systems," *Microwave Symposium Digest, 1999 IEEE*, vol.2, no., pp.467-470 vol.2, 1999.
- [2] D. Kuylenstierna, et.al., "Composite right/left handed transmission line phase shifter using ferroelectric varactors," *LMWC*, vol.16, no.4, pp. 167- 169, April 2006.
- [3] G.M. Rebeiz, et.al., "RF MEMS phase shifters: design and applications," *IEEE Microw. Mag.*, vol.3, no.2, pp.72-81, Jun 2002.
- [4] C.M. Andersson, et.al., "A SiC Varactor With Large Effective Tuning Range for Microwave Power Applications," *EDL*, vol.32, no.6, pp.788-790, June 2011.
- [5] M. Ozen, et.al., "High efficiency RF pulse width modulation with tunable load network class-E PA," *Proc. WAMICON*, pp.1-6, 18-19 April 2011.
- [6] R. Quaglia, et.al., "A double stub impedance tuner with SiC diode varactors," *Proc. APMC*, December 2011, Melbourne.
- [7] F. Ellinger, et.al., "Compact reflective-type phase-shifter MMIC for C-band using a lumped-element coupler," *MTT*, vol.49, no.5, pp.913-917, May 2001.
- [8] *3680 Series Universal Test Fixtures*, Anritsu/Wiltron, USA, August 1995.
- [9] G.F. Engen, C.A. Hoer, "Thru-Reflect-Line: An Improved Technique for Calibrating the Dual Six-Port Automatic Network Analyzer," *MTT*, vol.27, no.12, pp. 987- 993, Dec 1979.